IEEE Robotics and Automation Letters (RA-L) paper, presented at ICRA 2026, Vienna, Austria. Cite as RA-L paper.

Flexible-link velocity-bounding proxy based sliding mode control

Abstract— **This paper proposes a control strategy for flexible link manipulators preserving high tracking accuracy in free motion, while ensuring smooth and safe behavior in scenarios involving physical interaction or large positional errors, based on the VB-PSMC. The scheme is extended to compensate for the manipulator's flexural dynamics, resulting in a nested control scheme where damping of the induced oscillations is achieved by a model-free proportional strain feedback while gravity induced deflections are counteracted by a feed-forward term based on a quasi-static Euler-Bernoulli beam model. A convergence study on the modified sliding manifold and a stability analysis of the closed-loop system is provided. The performance of the controller was evaluated experimentally and compared against other control strategies such as PSMC and torque limited PD control. The results demonstrate the controller's accurate end effector tracking in free motion, while achieving compliant behavior during contact, by efficiently handling the link's inherent flexibility leading up to a 32% reduction in interaction force. In addition, studying the FL-VB-PSMC response after releasing contact demonstrated the smooth and vibration-free recovery even for large position errors.**

I. INTRODUCTION

Flexible link robots, characterized by reduced rigidity and lightweight design exhibit inherent compliance, which is interesting in the scope of collaborative robotics. However, the same flexibility introduces significant control challenges, including oscillations, deflections and complex coupled dynamics. Li et al. [1] and Subedi et al. [2] provide two of the most recent reviews on control strategies for flexible link manipulators (FLM), from which it becomes clear that the vast majority of the works focus on mitigating link-induced oscillations and achieving precise end-effector tracking in free motion.

Various different position control approaches have been proposed, with recent advancements including model-free finite-time tracking [3], passivity-based adaptive control [4], and sliding mode control variants [5], often enhanced with neural networks [6] or learning-based schemes [7]. Boundary control approaches have been proposed by [8] and [9], while also deep reinforcement learning strategies for flexible link control have gained attention [10] [11].

However, in collaborative settings, addressing the challenges of the reduced structural rigidity while simultaneously guaranteeing safe interaction is crucial. While extensive compliant controllers for rigid and flexible joint robots have been designed [12], interaction control for FLM is relatively unexplored. Calanca et al. developed a PD force control for a 1 DOF flexible link manipulator [13], focussing on constrained motion. Payo et al., on the other hand, realize force control based on coupling torque feedback by integrating a collision detection algorithm to switch from one controller to another to handle both constrained and unconstrained motion [14]. Fayazi et al. proposed a fractional-order sliding mode control scheme integrated with a disturbance observer, to achieve robust impedance control of a single-link flexible robotic arm interacting with an unknown environment [15]. Yannick et al [16] proposed an alternative approach to impedance control, based on a closed-form output-redefined and perturbed dynamic model with a nested strategy. An inner Two-Time Scale Adaptive Robust Control loop ensures fast and precise motion, while an outer control loop guarantees the desired impedance behavior in constrained motion. As the above control strategies are model-based approaches, they require simplified models (truncated modes, linearized, or decoupled) as the dynamics of flexible-link manipulators are governed by fourth-order partial differential equations. Garant and Gosselin [17], on the other hand, proposed a proprioceptive sensing framework for safe whole-body interaction with flexible robots, without requiring full dynamic models, but did not address end-effector tracking.

Proxy-based Sliding Mode Control (PSMC) is an extension of force-limited PID control and a modified version of Sliding Mode Control (SMC) [18]. While traditional impedance and admittance based approaches inherently trade off compliance against tracking accuracy [19], PSMC enables overdamped recovery after actuator-force saturation without sacrificing responsive tracking during normal operations. The introduction of a proxy allows to suppress the chattering effects induced by sliding mode. While recent improvements such as adaptive integral SMC via singular perturbation [20] and robust terminal SMC [21] also significantly reduce chattering, the main advantage of the PSMC is the decoupling of local and global dynamics. The local dynamics (governing the response to small position errors) are managed by the virtual coupling defined through the PID gains, while the global dynamics (large position error/interaction) are determined by the sliding mode parameter, providing smooth and safe recovery during interaction. PSMC was extended to Velocity-Bounding PSMC (VB-PSMC), which allows an additional explicit constraint on the velocity [22]. While PSMC and VB-PSMC show interesting features in the context of collaborative robotics, they have not yet been applied to flexible-link manipulators. Therefore, this paper introduces Flexible-Link Velocity-Bounding Proxy-Based Sliding Mode Control (FL-VB-PSMC), the first extension of VB-PSMC explicitly designed to address the combined challenges of flexural dynamics and safe interaction. The proposed controller compensates for flexural dynamics and preserves high tracking accuracy in free motion, while ensuring smooth, safe, and robust recovery in scenarios involving physical interaction or large positional errors. In contrast to other approaches, the FL-VB-PSMC does not rely on a complex dynamic model, manages both free and

constrained motion without need for collision detection, and handles interactions anywhere along the link.

The main contributions of this paper are as follows:

- We extend VB-PSMC to flexible link manipulators, explicitly compensating for flexural effects.
- We establish the stability analysis of the proposed controller.
- We experimentally demonstrate that the proposed controller ensures accurate tracking in free motion while preserving safe interaction behavior, achieving up to a 32% reduction in interaction force compared to traditional controllers under identical test conditions.

The paper is organised as follows. Section II presents preliminaries on the considered system. Section III introduces the proposed extension of the VB-PSMC for flexible link manipulators, while section IV presents the stability analysis of the proposed controller. Section V details the experimental validation. Finally, section VI highlights the conclusions.

II. Preliminaries

The dynamics of a flexible-link manipulator are typically modeled using Euler–Bernoulli beam theory, assuming a cantilever beam and a discrete end-effector payload. Considering the scenario depicted in Fig. 1, with F_g and F_{PL} the gravitational force due to the link's self weight and the payload respectively, and F_{int} an interaction force along the link, the transverse deflection $v(x,t)$ at location x from the base at time instant t satisfies [24]:

$$\frac{EI_y}{\rho}\frac{\partial^4}{\partial x^4}v(x,t) + d_f\frac{\partial}{\partial t}v(x,t) + \rho\frac{\partial^2}{\partial t^2}v(x,t) = f_{ext}(x,t) \tag{1}$$

with f_{ext} the resulting external force density distribution, E and ρ the Young's modulus and density of the material, d_f the damping coefficient and I_y the area moment of inertia about the neutral axis of the cross-section. Using the assumed mode method as discretization technique, the deflection $v(x,t)$ is expressed as a linear combination of n mode shapes $\phi(x)$ and time-dependent generalized coordinates $\eta(t)$ [5]:

$$v(x,t) = \sum_{j=1}^{n} \phi_j(x)\eta_j(t) \tag{2}$$

By applying the Lagrangian approach and inserting eq. 2 and 1, the closed form dynamic equations can expressed in terms of the rigid coordinates θ and modal coordinates η [4]:

$$\begin{bmatrix} M_{rr}(\theta,\eta) & M_{rf}(\theta,\eta) \\ M_{fr}(\theta,\eta) & M_{ff}(\theta,\eta) \end{bmatrix} \begin{bmatrix} \ddot{\theta} \\ \ddot{\eta} \end{bmatrix} + \begin{bmatrix} C_r(\theta,\eta,\dot{\theta},\dot{\eta}) \\ C_f(\theta,\eta,\dot{\theta},\dot{\eta}) \end{bmatrix} \begin{bmatrix} \dot{\theta} \\ \dot{\eta} \end{bmatrix}$$

$$+ \begin{bmatrix} 0 \\ K\eta \end{bmatrix} + \begin{bmatrix} D_r \\ D_f \end{bmatrix} \begin{bmatrix} \dot{\theta} \\ \dot{\eta} \end{bmatrix} + \begin{bmatrix} G_r(\theta,\eta) \\ G_f(\theta,\eta) \end{bmatrix} = \begin{bmatrix} \tau \\ 0 \end{bmatrix} + \begin{bmatrix} \tau_{int,r} \\ \tau_{int,f} \end{bmatrix} \tag{3}$$

$M_{rr}, M_{rf}, M_{fr}, M_{ff}$ denote the rigid-rigid, rigid-flexible, flexible-rigid, and flexible-flexible components of the inertia matrix, C_r, C_f denote the Coriolis and centrifugal force vectors. K represents the modal stiffness matrix while D_r and D_f are the joint and structural damping matrices and G_r, G_f the gravitational forces. τ represent the actuator torques, while $\tau_{int,r}$ and $\tau_{int,f}$ represents the interaction torques projected on the rigid and flexible coordinates respectively [4]. It is worth mentioning that the proposed controller does not explicitly rely on the derived dynamic model.

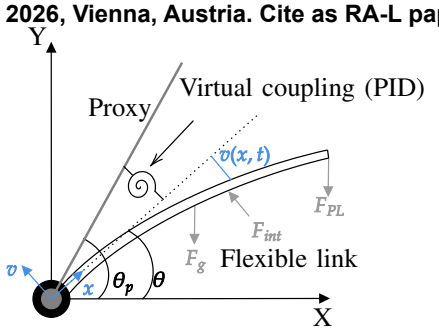

Fig. 1. Visualization of the considered scenario: the flexible link manipulator is subject to gravity and features a payload at the end. F_{int} represents an interaction force at a random position along the link. In addition, the principle of the proxy acting on the flexible link in joint space is visually represented (cf. Section III)

III. Flexible-link VB-PSMC

To realize safe yet accurate end effector tracking, we propose a nested control strategy based on the joint space implementation of a VB-PSMC. The original scheme, proposed by Kikuuwe [22], is extended to handle the undesired side effects of the reduced link rigidity. The resulting control architecture, called FL-VB-PSMC, is visualised in Fig. 2. In specific, vibration control, shown in orange, is implemented through proportional strain feedback, while gravity-induced deflections are compensated using a feed-forward term based on a static model, represented by the blue region in Fig. 2. Details of the different control loops are provided in the following subsections.

A. Joint control

Angular joint position control is achieved using velocity-bounding proxy-based sliding mode control, as depicted in Fig. 2. VB-PSMC was originally introduced by Kikuuwe in task-space formulation [22]. However, as the proposed FL-VB-PSMC relies on the joint space implementation, this section details the principles of the controller accordingly.

The VB-PSMC framework is built on proxy-based sliding mode control [18], with the addition of a magnitude limit in the sliding manifold to ensure constrained velocities. This constraint prevents excessively large velocities that may arise when the positional error is high and the system has not yet reached the sliding manifold. This methodology keeps the capability of overdamped recovering motion from large positional errors without sacrificing tracking accuracy when the velocity is constrained [22].

The principle of VB-PSMC is illustrated in Fig. 1. The actual controlled object is connected to a virtual object which is referred to as a proxy using a virtual coupling (PID controller). The PID controller causes an interaction torque,

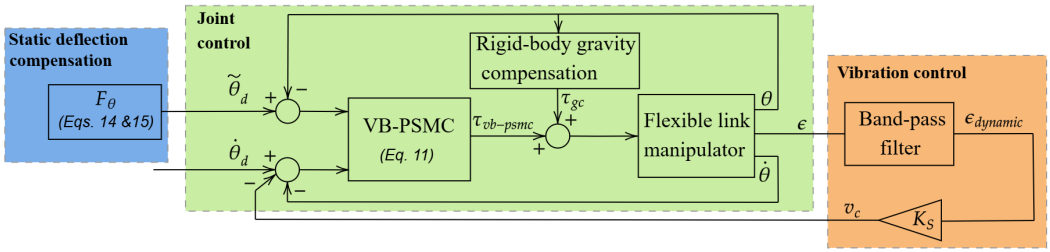

Fig. 2. Control scheme of the Flexible-Link Velocity-Bounding Proxy-Based Sliding Mode Control (FL-VB-PSMC) algorithm, including the VB-PSMC joint controller (green), which governs the motor and joint dynamics, a feedforward term that compensates for the static deflection induced by gravity (blue) and a vibration controller (orange), consisting of a proportional strain feedback.

τ_{pid}, between the end-effector and the proxy. At the same time, the proxy is controlled by a sliding controller which exerts a torque τ_c to track the desired trajectory. The proxy's equation of motion is governed by:

$$I_p\ddot{\theta}_p = \tau_c - \tau_{pid} \tag{4}$$

With I_p, the proxy's moment of inertia and $\ddot{\theta}_p$ the acceleration of the proxy. As shown in Fig. 1, θ_p and $\dot{\theta}_p$ are proxy's angular position and angular velocity while θ and $\dot{\theta}$ are the angular position and velocity of the controlled object.

The sliding mode control law used to control the virtual coupling is given by:

$$\tau_c = T \ \text{sgn(s)} \tag{5}$$

With the sliding surface, s, defined as:

$$s = V \,\text{sat}\left[\frac{\phi + \dot{\theta}_p}{V}\right] - \dot{\theta}_p \tag{6}$$

where:

$$\phi = A\left[\theta_d - \theta_p + H\left(\dot{\theta}_d - \dot{\theta}_p\right)\right] \tag{7}$$

With θ_d and $\dot{\theta}_d$ the desired angular position and velocity, and A an arbitrary positive value. T represents the imposed torque limit, V the maximum velocity in the controlled system, and H represents the time constant.

On the other hand, the torque produced by the PID controller with gains K_p, K_i and K_d is given by:

$$\tau_{pid} = K_p\left(\theta_p - \theta\right) + K_i\int\left(\theta_p - \theta\right)\,dt + K_d\left(\dot{\theta}_p - \dot{\theta}\right) \tag{8}$$

with θ and $\dot{\theta}$ angular position and angular velocity of the actual controlled object.

By introducing:

$$a = \int\left(\theta_p - \theta\right)\,dt \tag{9}$$

and setting $I_p = 0$ (*analogy of a massless proxy in task space*), eq. 4 implies that $\tau_{\text{vb-psmc}} = \tau_c = \tau_{pid}$ and thus:

$$\begin{aligned}\tau_{\text{vb-psmc}} &= K_p\dot{a} + K_i a + K_d\ddot{a} = T\,\text{sgn}(s_p)\\ s_p &= V\,\text{sat}\left(\frac{\phi_p + \ddot{a} + \dot{\theta}}{V}\right) - \ddot{a} - \dot{\theta}\\ \phi_p &= A\left[(\theta_d - \theta) + H(\dot{\theta}_d - \dot{\theta}) - \dot{a} - H\ddot{a}\right]\end{aligned} \tag{10}$$

Using *Theorem 1* from [18], the torque produced by the virtual coupling and the sliding model is formulated as:

$$\begin{aligned}\tau_{\text{vb-psmc}} = T\,\text{sat}\Bigg[\frac{1}{T}\Bigg(K_d V\,\text{sat}\left(\frac{\phi_p + \ddot{a} + \dot{\theta}}{V}\right)\\ + K_i a + K_p\dot{a} - K_d\dot{\theta}\Bigg)\Bigg]\end{aligned} \tag{11}$$

As the system operates in the gravity field, the control law is extended with a model based gravity compensation term, τ_{gc}, accounting for the rigid-body gravitational torque.

B. Vibration control

Reducing link rigidity inevitably introduces oscillations, which must be mitigated to ensure accurate control. Therefore, a proportional strain feedback strategy, relying on strain gauge measurements along the link, is implemented [23]. In free motion, the strain at a distance x_s from the hub can be expressed as [24]:

$$\epsilon(x_s, p) = \underbrace{\sum_{j=1}^{n}\frac{k_{\text{dyn},j}\theta(p)p^2}{p^2 + D_{f,j}p + \omega_{0,j}^2}}_{\epsilon_{\text{dynamic}}} + \underbrace{\sum_{j=1}^{n}\frac{k_{\text{stat},j}}{p^2 + D_{f,j}p + \omega_{0,j}^2}}_{\epsilon_{\text{static}}} \tag{12}$$

with p the Laplace variable, $\omega_{0,j}$ the j-th eigenfreqency and $D_{f,j} = 2\zeta_j\omega_{0,j}$ with ζ_j the j-th modal damping ratio. $k_{dyn,j}$ is the dynamic modal gain and accounts for the effect of the joint acceleration while the static modal gain $k_{stat,j}$ represents the influence of the gravity. To achieve vibration control via direct strain feedback, the dynamic component of the strain is used as the error signal in a proportional controller. Because the vibrational energy is predominantly concentrated in the first mode [23], it is sufficient to only consider the frequency components of the strain signal in the vicinity of the fundamental natural frequency $\omega_{0,1}$ [1]. To this end, the strain signal is processed with a Butterworth band-pass filter centered around $\omega_{0,1}$, which effectively suppresses the static component and isolates the oscillatory dynamics necessary for vibration suppression. As for human interactions, the associated frequency content is expected to remain below 2.3 Hz [17], the corresponding quasi-static

[1]For the considered setup in section V, $f_{0,1} = \omega_{0,1}/2\pi = 6.5$ Hz.

strain components are equally suppressed by the lower cutoff frequency, while high-frequency disturbances, e.g. induced by collisions, are attenuated by the upper cutoff frequency.

The strain feedback strategy can be inserted at different locations of the joint control, more specifically at the joint velocity, joint position and torque level. To determine the optimal insertion point for the proportional strain feedback, the root locus of these three strategies was analyzed. Strain feedback inserted at the velocity level appeared to have the highest damping potential, while being most robust to peak strain values experienced during highly dynamic motion.

C. Deflection compensation

In addition to dynamic vibrations, flexible links are subject to gravitational deflections which require compensation. To address this, a model-based feed-forward compensation term is designed. As vibrations are suppressed within the strain feedback loop, the resulting control loop does not require the integration of the complete dynamic model as derived in section II. For the quasi-static case, eq. 1 reduces to:

$$\frac{d^2 v_{stat}}{dx^2} = \frac{M_b(x)}{E \cdot I_y} \tag{13}$$

with $M_b\,(x)$ the internal moment distribution at distance x along the beam. For the cantilever beam considered in Fig 1, with length L and clamped at an angle θ, the internal moment distribution caused by gravity equals [23]:

$$\begin{aligned} M_b(x) = &-\left(\tfrac{F_g L}{2} + F_{PL} L\right)\cos\theta \\ &+ \left(F_g + F_{PL}\right) x \cos\theta - \tfrac{F_g x^2}{2L}\cos\theta \end{aligned} \tag{14}$$

By substituting eq. 14 into eq. 13 and performing a double integration, the static deflection v_{stat} at the tip of the link can be determined. Multiplying this value by $cos(\theta)$ yields v_z, the vertical offset that should be added to the desired position in Cartesian space. As the designed controller is operating in joint space, the corresponding joint angle offset, θ_e, is computed and added to the desired joint angle θ_d to obtain the reference for the VB-PSMC, $\tilde{\theta}_d$:

$$\tilde{\theta}_d = \theta_d + \theta_e \tag{15}$$

D. Convergence analysis

The contribution of the strain feedback affects the control law of the VB-PSMC, leading to a modified sliding manifold. By considering v_c as the contribution from the strain feedback control, the sliding manifold s_p becomes:

$$s_p = V \,\mathrm{sat}\left(\frac{\phi_p + \ddot{a} + \dot{\theta}}{V}\right) - \ddot{a} - \dot{\theta} \tag{16}$$

where

$$\phi_p = A\left[(\theta_\mathrm{d} - \theta) + H\left(\dot{\theta}_\mathrm{d} + v_\mathrm{c} - \dot{\theta}\right) - \dot{a} - H\ddot{a}\right]. \tag{17}$$

Differentiating eq. 16 yields to :

$$\dot{s}_p = \mathrm{sat}'\left(\frac{\phi_p + \ddot{a} + \dot{\theta}}{V}\right)\left(\dot{\phi}_p + \dddot{a} + \ddot{\theta}\right) - \ddot{a} - \ddot{\theta} \tag{18}$$

By considering the Lyapunov candidate function:

$$V_\sigma = \frac{1}{2} s_p^2 \tag{19}$$

whose time derivative is:

$$\begin{aligned} \dot{V}_\sigma &= s_p \dot{s}_p \\ &= s_p\left[\mathrm{sat}'\left(\frac{\phi_p + \ddot{a} + \dot{\theta}}{V}\right)\left(\dot{\phi}_p + \dddot{a} + \ddot{\theta}\right) - \dddot{a} - \ddot{\theta}\right]. \end{aligned} \tag{20}$$

Using the triangular inequality, eq. 20 is formulated as:

$$|\dot{V}_\sigma| \le \|s_p\|\left|\mathrm{sat}'\left(\frac{\phi_p + \ddot{a} + \dot{\theta}}{V}\right)\right|\|\dot{\phi}_p\| + \|\dddot{a} + \ddot{\theta}\| + \|s_p\|\|\dddot{a} + \ddot{\theta}\| \tag{21}$$

Assuming that the saturation function is Lipschitz continuous (i.e., $\mathrm{sat}'(x) \le M$) :

$$|\dot{V}_\sigma| \le \|s_p\|\Big[M\big(\|\dot{\phi}_p\| + \|\dddot{a} + \ddot{\theta}\|\big) + \|\dddot{a} + \ddot{\theta}\|\Big]. \tag{22}$$

Torques and references are bounded so that $\|\dddot{a} + \ddot{\theta}\| < \mu T$, which leads to:

$$|\dot{V}_\sigma| \le \|s_p\|\Big[M\|\dot{\phi}_p\| + (M+1)\mu T\Big] \tag{23}$$

with $\mu > 1$. Defining $\lambda := M\|\dot{\phi}_p\| + (M+1)\mu T$ and applying Young's inequality to eq. 23 yields:

$$\dot{V}_\sigma \le -\alpha\|s_p\|^2 + \beta \tag{24}$$

with $\beta := \frac{\lambda^2}{2\alpha}$ and $\alpha > 0$. This inequality implies that $\dot{V}_\sigma < 0$ whenever $\|s_p\|^2 > \frac{\beta}{\alpha}$, ensuring that the Lyapunov function decreases outside a compact set. Consequently, the sliding variable s_p is ultimately bounded and satisfies:

$$\|s_p(t)\| \le \frac{\lambda}{\sqrt{2\alpha}}, \quad \text{as } t \to \infty \tag{25}$$

This guarantees that the system trajectories converge to a neighborhood of the sliding manifold $s_p = 0$, with the radius of the neighborhood ($\frac{\lambda}{\sqrt{2\alpha}}$) characterized by the control gains (A and H) and the torque limit T. This result confirms the convergence of the sliding motion in the presence of bounded strain feedback.

IV. Stability analysis

We analyze the stability of the closed loop system using an interconnected system framework, composed of:

- Subsystem I : The flexible link manipulator controlled by VB-PSMC, without strain feedback.
- Subsystem II : Strain feedback control, inserted at the velocity level of VB-PSMC.

A. *Subsystem* I

Considering a composite storage Lyapunov function :

$$V_1 = V_{\mathrm{E}} + V_\sigma \tag{26}$$

with :

$$V_{\mathrm{E}} = \tfrac{1}{2}\,\dot{q}^\top M(q)\dot{q} + \tfrac{1}{2}\,\eta^\top K\eta \qquad V_\sigma = \tfrac{1}{2}\,s_p^2 \tag{27}$$

where $q = \begin{bmatrix}\theta \\ \eta\end{bmatrix}$, $M(q) = \begin{bmatrix}M_{rr} & M_{rf} \\ M_{fr} & M_{ff}\end{bmatrix}$.

Obviously, V_1 is positive definite. Differentiating V_{E} and reorganizing the terms yields [4] :

$$\dot{V}_{\mathrm{E}} = \dot{\theta}^T\tau_{\text{vb-psmc}} + \frac{1}{2}\dot{q}^T\left[\dot{M}(q) - 2\,C(q)\right]\dot{q} - \tfrac{1}{2}\dot{\theta}^T D_r\dot{\theta} - \dot{\eta}^T D_f\dot{\eta} \tag{28}$$

As the control input is bounded by the torque limit, using the property of skew-symmetry matrix and Rayleigh quotient inequality, eq. 28 is expressed as:

$$\dot{V}_{\mathrm{E}} \le -\tfrac{1}{2}\dot{\theta}^T D_r\dot{\theta} - \dot{\eta}^T D_f\dot{\eta} + \tfrac{1}{2}T^2\lambda_{\max}(D_r^{-1}) \tag{29}$$

As shown in Section III-D, differentiating V_σ yields:

$$\dot{V}_\sigma \le -\alpha\|s_p\|^2 + \beta. \tag{30}$$

Combining eq. 29 and eq. 30 gives:

$$\dot{V}_1 \le -\alpha_1\|x_1\|^2 + \beta_1 \tag{31}$$

with:

$$\begin{cases} x_1 := \begin{bmatrix}\dot{\theta} & \dot{\eta} & s_p\end{bmatrix}^T \\ \alpha_1 = \min\left\{\tfrac{1}{2}\lambda_{\min}(D_r),\ \lambda_{\min}(D_f),\ \alpha\right\} \\ \beta_1 = \tfrac{1}{2}T^2\lambda_{\max}(D_r^{-1}) + \beta \end{cases}$$

This inequality implies that Subsytem I is uniformly ultimately bounded, with radius proportional to $\sqrt{\beta_1/\alpha_1}$, which depends on the controller gains.

B. *Subsystem* II

The strain feedback control is inserted at the velocity level, with a signal defined as:

$$v_c = K_s H(s)\epsilon \tag{32}$$

where $H(s)$ is a stable second-order Butterworth band-pass filter, K_s the strain feedback gain and ϵ is the measured strain along the flexible link. The strain is a bounded signal, induced by the motion of the flexible-link manipulator, governed by Subsystem I, whose state is denoted by x_1 : $\|\epsilon\| \le c_\epsilon\|x_1\|$, with $c_\epsilon > 0$ (cf. Fig. 2).

Since $H(s)$ is stable and fast, the strain feedback is approximated as a static gain operator:

$$\|v_c\| \;\le\; |K_s|\|H\|_\infty\|\epsilon\| \;\le\; c_{vc}\,\|x_1\| \tag{33}$$

with $c_{vc} := |K_s|\|H\|_\infty c_\epsilon$. Hence Subsystem II is ISS with respect to x_1, with finite gain $\gamma_2 = c_{vc}$ [26].

C. *Closed loop*

For the interconnected case, Subsystem I can be equivalently expressed in input-to-state stable (ISS) form with respect to v_c, with finite gain $\gamma_{12} > 0$ [25] :

$$\dot{V}_1 \le -\alpha_1\|x_1\|^2 + \gamma_{12}\|v_c\|^2 + \beta_1. \tag{34}$$

By defining the interconnected gain, γ_1, as $\gamma_1 := \sqrt{\frac{\gamma_{12}}{\alpha_1}}$ and substituting eq. 33 into eq. 34, it leads to:

$$\dot{V}_1 \le -\alpha_1(1 - (\gamma_1\gamma_2)^2)\|x_1\|^2 + \beta_1. \tag{35}$$

By selecting K_s such as, $|K_s| < \frac{1}{\|H\|_\infty c_\epsilon}\sqrt{\frac{\alpha_1}{\gamma_{12}}}$, $\gamma_1\gamma_2 < 1$ holds. By the small gain theorem, the closed-loop system is uniformly ultimately bounded, with ultimate bound $\|x_1(t)\| \le \sqrt{\frac{\beta_1}{\alpha_1(1-(\gamma_1\gamma_2)^2)}}$. Therefore, all trajectories converge to a compact set around the origin, whose size depends on the controller gains.

V. Experimental validation

A. *Experimental setup and implementation*

The experimental setup consists of a single link FLM made of a rectangular aluminum beam with a length of 0.5 m. The link is actuated by an EC Maxon motor equipped with integrated gearbox and an incremental encoder. A set of strain gauges is placed at a distance $x_s = 0.05$ m from the motor hub. The strain signals are acquired using a Beckhoff data acquisition system and processed alongside motor data in MATLAB Simulink through the TwinCAT environment, operating at a sampling frequency of 1 kHz. The experimental setup is depicted in Fig. 3.

The tuning of FL-VB-PSMC was performed in different steps. First, the local dynamics (governed by the PID) were tuned based on Ziegler-Nichols tuning with a follow-up refinement to make the controller less aggressive. Then, the global dynamics gains were tuned following the guidelines stated in [18], with additional experiments assessing their influence within the prescribed ranges. Specifically, the local gains were selected as $K_p = 150$, $K_i = 15$ and $K_d = 6.5$, while the global parameters were set as follows: T = 7.9 Nm, V = 3 rad/s, and H = 0.1 s. Finally, the strain feedback gain was selected by investigating the system's root locus, resulting in the gain $K_s = 3500$.

B. *Free motion - Trajectory tracking*

A series of experiments were conducted to evaluate the tracking accuracy of the FL-VB-PSMC in free motion. The performance of the controller was assessed by tracking the end-effector position using a Vicon motion capture system, by analyzing the dynamic strain data and inspecting the joint velocity. A payload of 0.02 kg, corresponding to a payload-to-linkmass ratio of 0.4, was attached at the free end of the flexible link. Videos of the experimentals are available here[2].

Fig. 4 (a) visualizes the vertical end-effector position captured by the Vicon system. The orange signal corresponds

[2]https://anonymous.4open.science/r/ExperimentalTests-6DE6/README.md

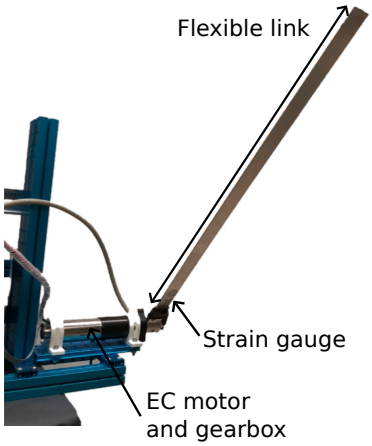

Fig. 3. Experimental setup consisting of a flexible link with rectangular cross section, with a pair of strain gauge mounted close to the base. The flexible link is actuated by a EC maxon motor with integrated gearbox.

to the case without vibration control and the static deflection compensation, while the dashed green represents the vertical coordinate when the vibration control is activated. The controller effectively suppresses oscillations, except for a small overshoot due to the high peak present in the dynamic strain, as illustrated in Fig. 4 (b). A static error induced by gravity is observed. However, when the deflection compensation is activated, as illustrated by the solid green line, the end-effector follows the reference with a max error of 2 mm. This highlights the effective implementation of the feedforward term, which successfully predicts the resulting deflection based on the applied load and the desired configuration. Fig. 5 depicts the joint velocity profile. It can be observed that when the desired velocity exceeds the velocity limit, the actual velocity remains constrained, illustrating the effect of the boundary layer on the sliding manifold (cf. eq. 10).

C. Safe response

To evaluate the controller's performance during and after interaction with the environment, two sets of experiments were conducted. The first experiment considers a collision scenario in which the tip of the flexible link manipulator impacts a load cell during motion for a few seconds. Once the obstruction is removed from the trajectory, the system's recovery towards the reference is analyzed in detail. The results obtained with the FL-VB-PSMC with a velocity limit of 5 rad/s and 3 rad/s are compared with those obtained with a regular PSMC and a torque limited PD controller, whereby a torque limit of 2 Nm was considered for all controllers.

Fig. 6 (a) visualizes the obtained joint response for the different controllers. During free motion, a satisfactory trajectory tracking is obtained with a response time that tends to be high because of the torque limit. It is also interesting to mention that the joint response obtained with the FL-VB-PSMC (V = 3), depicted in green, exhibits a slight delay compared to the other controllers, due to the additional constraint imposed by the velocity boundary layer. This is emphasized in Fig. 6 (b) where the velocity is constrained as soon as it reaches the limit, 3 rad/s, while for the case of PMSC and PD-sat, the joint velocity reaches 5.3 rad/s.

During collision, it can be observed that the flexible link deforms less when controlled by the FL-VB-PSMC, compared to the other controllers, whereby lowering the velocity limit tends to decrease the amount of link deformation. This is reflected in Fig. 6 (d), visualising the difference in measured strain values, as well as in Fig. 6 (a), highlighting the difference in the reached joint angle for the same position of the obstruction at the end effector. The velocity boundary layer therefore leads to a higher degree of active compliance, which is also reflected in the contact force measurements as shown in Fig. 6 (c), where the FL-VB-PSMC with V=3 results in a 32% reduction in the normal contact force relative to the PD-Sat controller.

After the release of the load cell, both PSMC and FL-VB-PSMC present an overdamped joint response, whereas the PD-sat results in a more aggressive and oscillatory joint response. In both regular PSMC and FL-VB-PSMC, the proxy is controlled via sliding mode control as it is pulled away from the reference because of the large positional error. As a result, the proxy starts moving towards the reference. When it reaches the sliding surface, it starts an exponential convergence, governed by the parameter H towards the desired position. The overdamped response is therefore guaranteed thanks to sliding mode, without compromising the tracking accuracy as the virtual coupling (PID) takes over the control of the joint angle once the proxy reaches the sliding surface. As demonstrated above (Fig. 4), despite the overdamped joint response, regular PSMC does not manage to counteract the flexural effects, while our FL-VB-PSMC manages to do so. FL-VB-PSMC therefore demonstrates to be a suitable (interaction) controller for flexible link manipulators, as it enables accurate end effector tracking in free motion, while achieving compliant behavior during contact, by efficiently handling the link's inherent flexibility.

To demonstrate the controller's response to human interactions, in a subsequent experiment, the manipulator was instructed to follow a reference trajectory while its motion was perturbed by a human at random locations along the link. Fig. 7 visualizes the desired and actual end-effector position, depicted respectively in dashed black and blue, as well as the interaction force (green). A video of the experiment can be found here [3]. Regions A and B on Fig. 7 correspond to interactions applied at different locations along the link, while in region C a cyclic interaction was induced at the tip. It can be seen that the controller reacts compliantly to all interactions, while converging smoothly back to the desired trajectory when releasing contact. In specific, this behavior is clearly depicted at the end of region B. Despite the large positional error originating from the human interaction (reaching up to $\pm 144^{\circ}$, corresponding to nearly $1\mathrm{m}$ at the end-effector), the end-effector smoothly returns to the desired reference, with an overdamped and vibration-free recovery motion. This highlights the safe and stable response of the

[3] https://anonymous.4open.science/r/ExperimentalTests-6DE6/README.md

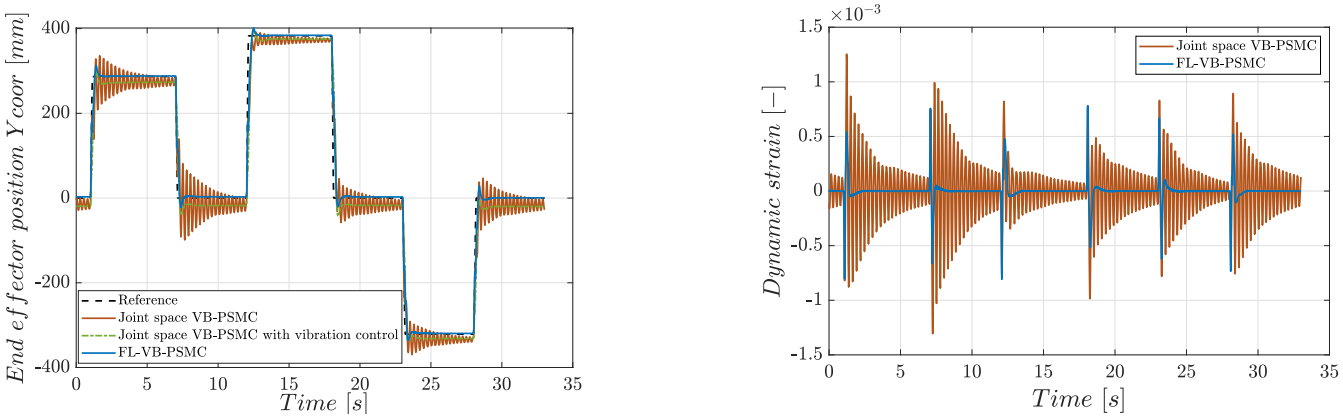

Fig. 4. Evaluation of the FL-VB-PSMC in free motion for different step-like trajectories with a payload of 0.02 kg (payload-to-mass ratio of 0.4). (a) End effector position. Dashed black: desired reference. Orange: regular VB-PSMC. Dashed green: VB-PSMC with vibration control. Blue: FL-VB-PSMC. (b) Dynamic strain. Blue: strain with FL-VB-PSMC. Orange: without vibration control.

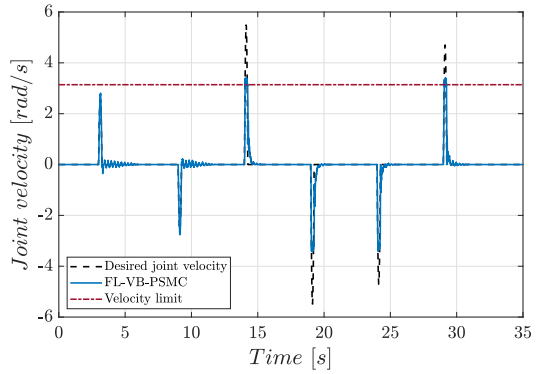

Fig. 5. Evaluation of the FL-VB-PSMC in free motion for different step-like trajectories with a payload of 0.02 kg: joint velocity. Dashed red: Velocity limit. Dashed black: desired velocity. Blue: measured joint velocity.

proposed FL-VB-PSMC upon interaction conditions.

VI. Conclusion

This paper presents a novel control strategy, called FL-VB-PSMC, designed to address the challenges induced by flexible link manipulators, ensuring high tracking accuracy while ensuring safe response during contact and large positional errors. The control architecture integrates three main components: a joint-level VB-PSMC, a proportional strain feedback loop for vibration control and a feedforward term, based on Euler-Bernouilli beam theory, to counteract gravity-induced deflections. A stability analysis confirms that the closed-loop system is uniformly ultimately bounded. Experimental validation on a single-link flexible link manipulator demonstrated the effectiveness of the controller to obtain accurate end-effector tracking in free motion and highlighted its overdamped response at large positional errors. Furthermore, comparative analysis with conventional PSMC and torque limited PD controllers indicated the enhanced compliance of the FL-VB-PSMC, with a 32 % reduction in contact force for the considered scenario. The integration of the velocity boundary layer results in a higher level of active compliance as the internal deformation of the link at collision is reduced, resulting in a reduced contact force during interaction. Future work includes extending FL-VB-PSMC to an adaptive controller to make it robust to changes in operating conditions and as well as to allow modification of the desired end effector behavior by properly adapting the local, global and vibration controller gains.

References

[1] Li, B., Li, X., Gao, H. & Wang, F. Advances in Flexible Robotic Manipulator Systems — Part II: Planning, Control, Applications, and Perspectives, *IEEE/ASME Transactions On Mechatronics*, 2024.

[2] D. Subedi, I. Tyapin, & G. Hovland, "Review on modeling and control of flexible link manipulators", *Modeling, Identification and Control: A Norwegian Research Bulletin*, 2020.

[3] Yang, Y., Su, Q., Hui, W., Li, J. & Ge, C, "Adaptive model-free finite-time tracking control for flexible-link manipulator with parametric and non-parametric uncertainties", *Nonlinear Dynamics*, 2025.

[4] Belherazem, A. & Chenafa, M., "Passivity Based Adaptive Control of a Single-Link Flexible Manipulator", *Automatic Control And Computer Sciences*, 2021.

[5] Belherazem, A., Salim, R., Laidani, A. et al. "Vibration Control of a Two-Link Flexible Manipulator",*Aut. Control Comp. Sci.*,2024.

[6] Lima, G., Porto, D., Oliveira, A. & Moreira Bessa, W., "Intelligent control of a single-link flexible manipulator using sliding modes and artificial neural networks", *Electronics Letters*, 2021.

[7] Zhi-Qiu, Jun-Hu & Xian-Zhang, "Multi-agent reinforcement learning vibration control and trajectory planning of a double flexible beam coupling system", *Mechanical Systems And Signal Processing*, 2023.

[8] Zhu J, Zhang J, Tang X, Pi Y, "Adaptive boundary control of a flexible-link flexible-joint manipulator under uncertainties and unknown disturbances",*Journal of Vibration and Control*, 2021.

[9] Zhao, Z., He, X. & Ahn, C., "Boundary Disturbance Observer-Based Control of a Vibrating Single-Link Flexible Manipulator", *IEEE Transactions On Systems, Man, And Cybernetics: Systems*, 2021.

[10] M. Sasaki, J. Muguro, F. Kitano, W. Njeri, D. Maeno, and K. Matsushita, "Vibration and position control of a two-link flexible manipulator using reinforcement learning,"*Machines*, 2023.

[11] Viswanadhapalli, J., Elumalai, V., S., S., Shah, S. & Mahajan, D., "Deep reinforcement learning with reward shaping for tracking control and vibration suppression of flexible link manipulator", *Applied Soft Computing*, 2024.

[12] Zhang, T., Du, Q., Yang, G., Chen, C., Wang, C. & Fang, Z., "A review of compliant control for collaborative robots", *2021 IEEE 16th Conference On Industrial Electronics And Applications (ICIEA)*, 2021.

[13] Calanca, A., Dimo, E., Vicario, R., Fiorini, P., Serpelloni, M. & Legnani, G., "Introducing Series Elastic Links for Affordable Torque-Controlled Robots", *IEEE Robotics And Automation Letters*, 2019.

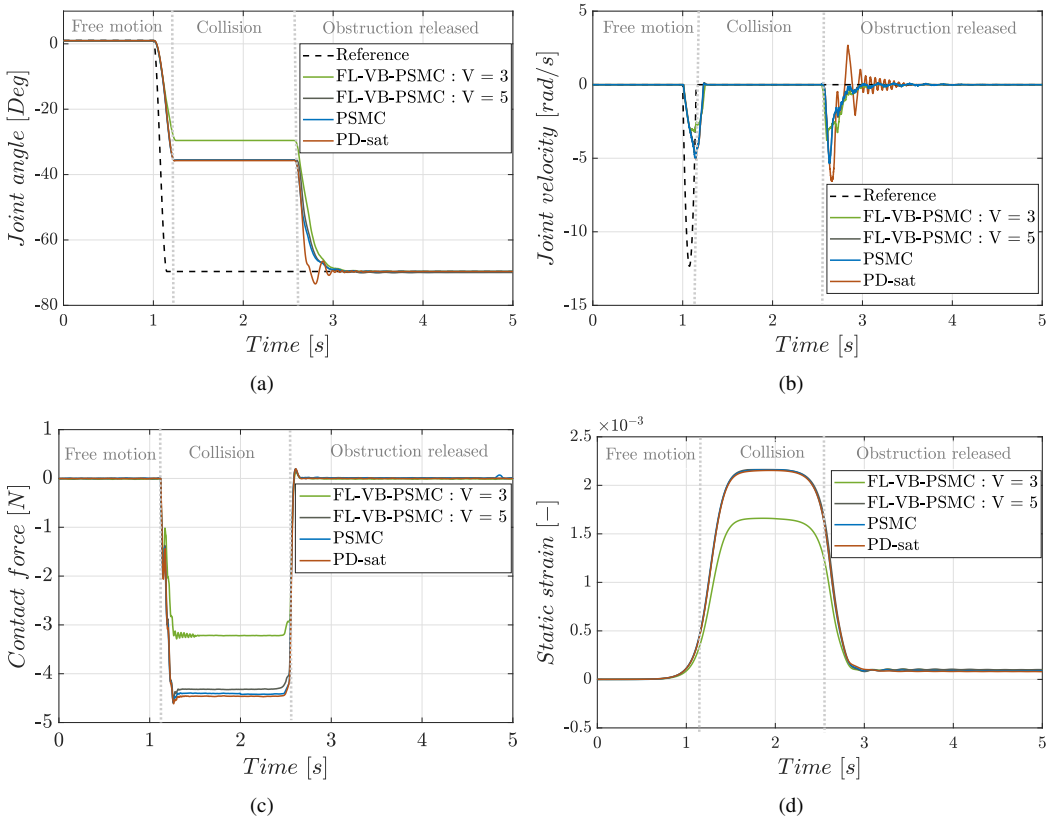

Fig. 6. Comparison of the performance of VB-PSMC, PSMC, and torque-saturated PD control during a collision event and after the release of the colliding object. (a) Joint angle, (b) Joint velocity, (c) Normal contact force, (d) Static strain.

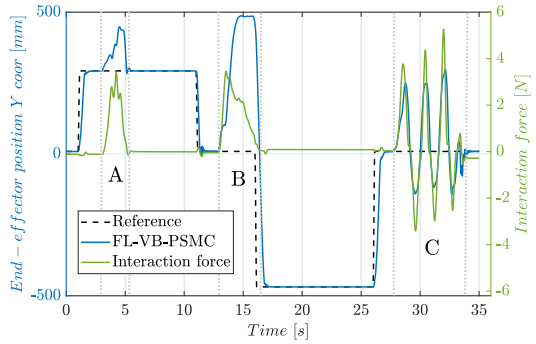

Fig. 7. End-effector position and interaction force upon physical interaction at random locations along the link, perturbing the initially predefined end-effector trajectory.

[14] Payo, I., Feliu, V. & Cortázar, O., "Force control of a very lightweight single-link flexible arm based on coupling torque feedback", *Mechatronics*, 2009.

[15] Fayazi, A., Pariz, N., Karimpour, A. & Hosseinnia, H., "Robust position-based impedance control of lightweight single-link flexible robots interacting with the unknown environment via a fractional-order sliding mode controller", *Robotica*, 2018.

[16] Cianyi, Y., Zhu, X. & Cao, J., "Adaptive Compliance Control of Flexible Link Manipulator in Unknown Environment", *International Conference on Intelligent Robotics and Applications*, 2022.

[17] Garant, X. & Gosselin, C, "Whole-Body Intuitive Physical Human-Robot Interaction With Flexible Robots Using Non-Collocated Proprioceptive Sensing", *IEEE Robotics And Automation Letters*, 2024.

[18] R. Kikuuwe and H. Fujimoto, "Proxy-based sliding mode control for accurate and safe position control", *IEEE International Conference on Robotics and Automation*, 2006.

[19] Schumacher, M., Wojtusch, J., Beckerle, P. & Von Stryk, O., "An introductory review of active compliant control", *Robotics And Autonomous Systems*, 2019.

[20] Khan, R., Rsetam, K., Cao, Z. & Man, Z. Singular Perturbation-Based Adaptive Integral Sliding Mode Control for Flexible Joint Robots. *IEEE Transactions On Industrial Electronics*, 2023.

[21] Rsetam, K., Cao, Z. & Man, Z. Design of Robust Terminal Sliding Mode Control for Underactuated Flexible Joint Robot. *IEEE Transactions On Systems, Man, And Cybernetics: Systems*, 2022.

[22] R. Kikuuwe, T. Yamamoto and H. Fujimoto, "Velocity-Bounding Stiff Position Controller", *IEEE/ International Conference on Intelligent Robots and Systems*, 2006.

[23] Van de Perre, G., Hubert, T., Verstraten, T. & Vanderborght, B., "Investigating the Potential of Flexible Links for Increased Payload to Mass Ratios for Collaborative Robotics", *IEEE Access*, 2023.

[24] Malzahn, J., "Modeling and control of multi-elastic-link robots under gravity", *PhD dissertation*, 2014.

[25] Khalil, H., "Nonlinear Systems", *Prentice Hall*, 2002.

[26] Sontag, E, "Input to state stability: Basic concepts and results", *Nonlinear And Optimal Control Theory*, 2008.